Stability Analysis of LCL-type Grid-Connected Inverters with Digital Delay based on Loop Gain Reconfiguration

Jiang Xin[1], Yi Hao[1], Li Yuguo[1], Zhuo Fang[1],Wang Feng[1] and Wang Zhenxiong[1]
[1] State Key Laboratory of Electrical Insulation and Power Equipment, Xi'an jiaotong University, China

***Abstract*-- Active damping is an effective method to suppress high frequency oscillation of LCL inverter. However, the digital control delay may introduce the right half plane poles into the control loop, which complicates the stability analysis and parameter design of the LCL inverter with active damping. Therefore, this paper proposed a loop gain reconfiguration method. With the proposed loop gain, the delay in the original loop gain denominator is cancelled to avoid the effect of right half plane poles on stability analysis. With the proposed loop gain, the analytic formula is derived to judge the stable range of the inverter. Based on the formula, the design method of the active damping gain and effect of delay and grid impedance on the stability are derived, which greatly simplifies the stability analysis and the parameter design of active damping.**

***Index Terms*-- LCL-type grid-connected converter, active damping, right half plane poles, loop gain reconfiguration.**

I. Introduction

With the great demand for renewable energy, the distributed generation technology has aroused great attention. Inverter plays an important role in the connection of distributed energy and grid. LCL filter has been widely used in grid-connected inverter for its small volume and stronger ripple attenuating ability compared with L filter. However, the resonance of LCL-filter has been an important concern for its application [1].

A variety of damping methods have been proposed with active damping (AD) methods studied more because passive damping methods will bring extra power loss [2]. The active damping methods can be generally divided into state-variable-feedback-based ones [3-15] and filter-based ones [16][17]. Among them, the filter capacitor current feedback (CCF) active damping has been widely studied for its simple implementation. [3-8]

The CCF active damping is, however, distorted by the delay in the digital system. The delay may add right-half-plane (RHP) poles to the system, which introduces a nonminimum-phase behavior to the system. It has been researched that the CCF with delay is equivalent to a virtual impedance in parallel with the capacitor and the virtual impedance may have a negative real part when the frequency is greater than one sixth of sampling frequency(f_s/6), which provides a negative damping and worsens the system stability.[3] Besides, it is also found that the system cannot keep stable no matter how the CCF is tuned when the LCL resonant frequency is equal to f_s/6.[5] In [4][7], condition of the RHP poles is analyzed in z-domain and the system stability is judged based on RHP poles, which need complicated analysis and the characteristic of LCL filter cannot be presented accurately in z-domain. In [6][8][18][19], the RHP poles are solved through compensating the digital delay, such as inserting a high-pass or lead-lag filter in the capacitor feedback loop, shifting the sampling time of the capacitor current. These methods are effective but neglect delay's positive effect on the stability because it has also been found that delay can provide inherent damping under certain circumstances.[20]

This paper proposed a loop gain reconfiguration method to avoid RHP poles without extra blocks or compensating the time delay. Based on the reconfigured loop gain, the delay and filter parameters effect on the stability can be mathematically analyzed. The stable regions presented as the value range of capacitor current feedback proportion are derived. Based on the analytic stable region formula, the effect of delay and grid impedance on the stable regions are derived, thus the stability of the inverter can be judged intuitively and the CCF be tuned easily. Simulation and experiment validated the effectiveness of the method.

II. Delay Effect on the System Stability

Fig.1 shows the topology and control block diagram of the LCL-Type Grid-Connected Inverter with CCF active damping. The phase-locked loop (PLL) is adopted

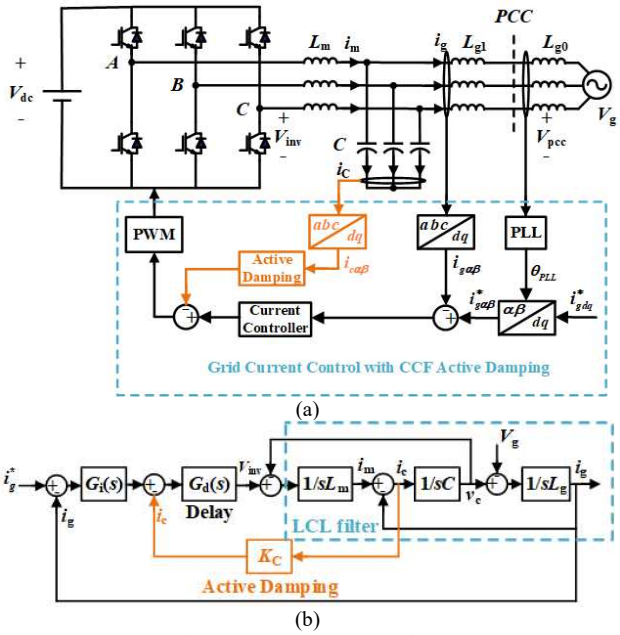

Fig. 1 LCL-type grid-connected converters with CCF active damping. (a)Three phase control scheme. (b) Per-phase block diagram

This paper is supported by the National Science Foundation of China (51977172).

to synchronize the converter with the point of common coupling (PCC) voltage. The grid voltage is assumed balanced so per-phase diagrams used for analysis can be depicted in Fig.1(b). The grid side inductor L_{g1} and grid inductance L_{g0} are combined together into L_g. The grid current i_g is fed back for regulation and capacitor current i_c is fed back with proportional gain of K_C to realize active damping. The current regulator $G_i(s)$ adopts proportional- resonant (PR) controller and can be simplified as a proportional gain of K_P near the resonant frequency of LCL filter.

Due to the reason that the resonant frequency of LCL filter is generally smaller than half of the switching frequency, thus the aliasing characteristic of current sampling and delay control can be neglected and the model can be built in the *s*-domain to better depict the characteristic of LCL filter. As mentioned before, digital control introduces computation delay and PWM delay to the system. The computation delay can be defined as $T_d = \lambda T_s$, T_s is one switching period. And $\lambda = 1$ when synchronous sampling is used [4]. In the *s*-domain, the computation delay can be expressed as (1)

$$G_{d1}(s) = e^{-\lambda T_s \cdot s} \tag{1}$$

The PWM delay can be modeled by zero-order-hold (ZOH). It has been proved that the delay caused by ZOH is relatively equal to a half sampling period [21]. Thus, the ZOH can be expressed as (2)

$$G_{d2}(s) = \frac{1 - e^{-T_s \cdot s}}{s} \approx T_s e^{-0.5 T_s \cdot s} \tag{2}$$

Therefore, the total digital control delay can be expressed as (3)

$$G_d(s) = e^{-(\lambda + 0.5) T_s \cdot s} \tag{3}$$

Referring to Fig.2, the loop gain of the grid current loop can be derived as (4).

$$\begin{aligned} T_1(s) &= \frac{K_P e^{-(\lambda+0.5)T_S \cdot s}}{s^3 L_m L_g C + s^2 L_g C K_C e^{-(\lambda+0.5)T_S \cdot s} + s(L_m + L_g)} \\ &= \frac{1}{s L_m L_g C} \cdot \frac{K_P e^{-(\lambda+0.5)T_S \cdot s}}{s^2 + \frac{K_C}{L_m} e^{-(\lambda+0.5)T_S \cdot s} \cdot s + \omega_r^2} \end{aligned} \tag{4}$$

Where ω_r is the LCL filter resonance angular frequency and can be expressed as (5).

$$\omega_r = \sqrt{\frac{L_m + L_g}{L_m L_g C}} = 2\pi f_r \tag{5}$$

It can be found that the delay is introduced to the denominator of the loop gain and that may lead to RHP poles, the aforementioned methods have to analyze the stability based on the judgement of RHP poles, which complicate the analysis process. However, if the term with delay doesn't appear on the denominator, the RHP poles can be avoided.

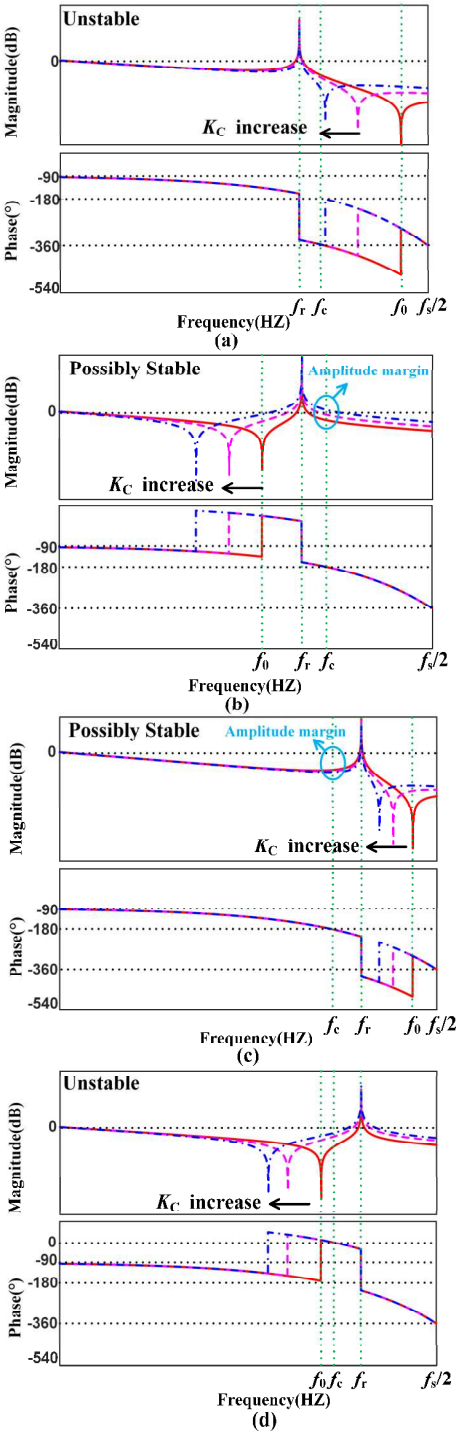

Fig. 2 Bode diagram of loop gain. (a) $f_r < f_c, f_r < f_0$. (b) $f_r < f_c, f_r > f_0$. (b) $f_r > f_c, f_r < f_0$. (d) $f_r > f_c, f_r > f_0$

III. Loop Gain Reconfiguration to Avoid RHP Poles

According to the *Automatic control theory*, the most fundamental stability criterion is that there is no right half plane root for system characteristic equation. And the stability analysis based on loop gain is developed from the fundamental criterion. The relationship between system characteristic equation and loop gain can be illustrated by (6).

$$1+T(s)=0 \tag{6}$$

Equation (6) represents the system characteristic equation while the T(s) represents the loop gain. That means the loop gain can have various forms and can be restructured only the form can satisfy equation (6). According to Fig.1(b), the system characteristic equation can be derived as (7).

$$\begin{aligned} &s^3L_{\mathrm{m}}L_{\mathrm{g}}C+s^2L_{\mathrm{g}}CK_Ce^{-(\lambda+0.5)T_{\mathrm{S}}\cdot s} \\ &+s\left(L_{\mathrm{m}}+L_{\mathrm{g}}\right)+K_Pe^{-(\lambda+0.5)T_{\mathrm{S}}\cdot s}=0 \end{aligned} \tag{7}$$

It can be found that (4) can be derived if '$s^3L_mL_gC+s(L_m+L_g)+s^2L_gCK_{PWM}K_Ce^{-(\lambda+0.5)T_s\cdot s}$'is divided on both sides of (7). Therefore, to avoid the term with delay on the denominator, the proposed loop gain can be derived by dividing '$s^3L_mL_gC+s(L_m+L_g)$' on both sides of (7) and can be expressed as (8).

$$\begin{aligned} T_2(s)&=\frac{s^2L_{\mathrm{g}}CK_C+K_P}{s^3L_{\mathrm{m}}L_{\mathrm{g}}C+s\left(L_{\mathrm{m}}+L_{\mathrm{g}}\right)}e^{-(\lambda+0.5)T_{\mathrm{S}}\cdot s} \\ &=\frac{K_C}{sL_m}\cdot\frac{s^2+\dfrac{K_P}{L_{\mathrm{g}}CK_C}}{s^2+\omega_{\mathrm{r}}^2}e^{-(\lambda+0.5)T_{\mathrm{S}}\cdot s} \end{aligned} \tag{8}$$

Because (4) and (8) both satisfy the form of equation (6), they are equivalent for stability analysis. And it can be found that there is no delay in the denominator of (8) thus the open loop RHP poles are avoided and the delay will only lead to system phase lag, which can greatly simplify the stability analysis.

According to (8), the bode diagram of the loop gain can be depicted in Fig.2. The figure is plotted with different capacitor current coefficient K_C. The black arrow in the figure indicates the direction where K_C increases. It can be found that there is a resonant peak with -180° phase jumping caused by the poles at the filter resonance frequency ω_r and a valley with 180° phase rising caused by the zeros at frequency ω_0, which can be expressed as (9).

$$\omega_0=\sqrt{\frac{K_P}{L_{\mathrm{g}}CK_C}}=2\pi f_0 \tag{9}$$

It can be found that ω_0 can be adjusted by K_C. Besides, the phase lag caused by the delay is equal to 90° at the frequency ω_c, which can be derived from (10).

$$(\lambda+0.5)T_s\cdot\omega_c=\frac{\pi}{2}\Rightarrow\omega_c=\frac{\omega_s}{4\lambda+2}=2\pi f_c \tag{10}$$

It can be derived from (10) that ω_c is equal to $\omega_s/6$ when $\lambda=1$, which has been regarded as a crucial frequency related with stability in previous studies. This paper shows that ω_c is actually the critical frequency of ω_r.

To reveal the parameters' influence on the system stability, four cases in terms of the relation of ω_r, ω_c and ω_0 are depicted in Fig.2, where only the system in Fig.2(b) and Fig.2(c) can possibly keep system stable. It should be noted that only ω_0, among the three frequencies, can be adjusted by K_C and K_P for a given system, which can be used to stabilize the active damping system.

TABLE I
SIMULATION AND EXPERIMENT PARAMETERS

Parameter	*Symbol*	*Value*
Inverter-side inductor	L_{m}	1.2mH
Grid-side inductor	L_{g1}	90μH
Filter capacitor	C	31μF
Grid inductance	L_{g0}	170μH
Resonant frequency	f_{r}	1.955kHZ
Switching frequency	f_{sw}	10kHZ
Sampling frequency	f_{s}	10kHZ
Computation delay coefficient	λ	1.5
Frequency of 90° phase lag by delay	f_{c}	1.25kHZ
Current regulator proportion	K_{P}	3
DC-link voltage	V_{dc}	800V
Grid voltage	V_{g}	311V

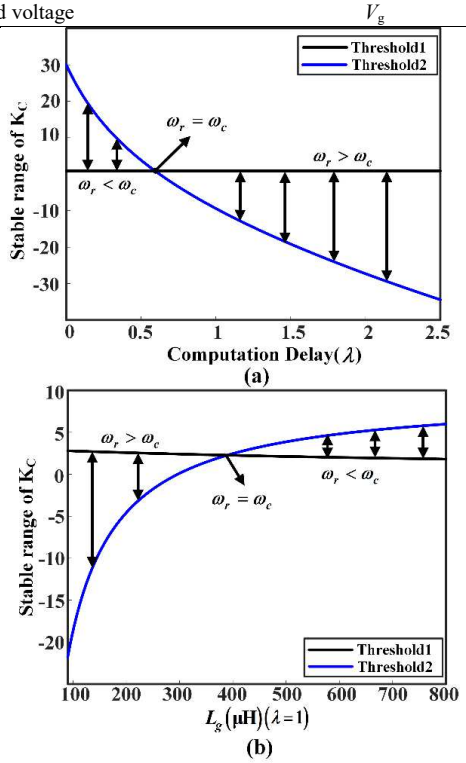

Fig. 3: Stable region of LCL-type grid-connected converters with CCF active damping. (a) Delay effect on stable region. (b) Grid inductance effect on stable region

In Fig.2(b), because $\omega_r>\omega_0$, the 180° phase rising at frequency ω_0 help avoid -180° phase crossing at the resonance peak, the phase will cross -180° at the frequency ω_c. The system can keep stable when the amplitude at the frequency ω_c is smaller than 0dB. Therefore, the value range of K_C to keep system stable when $\omega_r<\omega_c$ can be derived in (11)

$$\frac{K_P}{L_{\mathrm{g}}C\omega_r^2}<K_C<\frac{(4\lambda+2)^2K_P}{L_{\mathrm{g}}C\omega_s^2}-\frac{(4\lambda+2)\omega_{\mathrm{r}}^2L_{\mathrm{m}}}{\omega_s}+\frac{\omega_sL_{\mathrm{m}}}{(4\lambda+2)} \tag{11}$$

In Fig.2(c), because $\omega_r<\omega_0$, the phase lag larger than 90° can help avoid -180° phase crossing at the resonance peak. The phase will cross -180° at the frequency ω_c. The system can keep stable when the amplitude at the frequency ω_c is smaller than 0dB. Therefore, the value range of K_C to keep system stable when $\omega_r>\omega_c$ can be derived in (12).

$$\frac{(4\lambda+2)^2 K_P}{L_g C\omega_s^2}-\frac{(4\lambda+2)\omega_r^2 L_m}{\omega_s}+\frac{\omega_s L_m}{(4\lambda+2)}<K_C<\frac{K_P}{L_g C\omega_r^2} \quad (12)$$

Especially, when $\omega_r = \omega_0$ the resonant peak and valley are cancelled with each other and the loop gain is reduced from the third-order system to the first-order system. In this condition, the value of K_C can be calculated as (13).

$$K_C = \frac{K_P}{L_g C\omega_r^2} \quad (13)$$

But it should be noticed that the system is critical stable in this condition and sensitive to the filter parameters. With (11) and (12), the effect of active damping and delay on system stability can be mathematically analyzed. Define the two thresholds of K_C as (14)

$$\begin{aligned} \text{ThreShold1} &= \frac{K_P}{L_g C\omega_r^2} \\ \text{ThreShold2} &= \frac{(4\lambda+2)^2 K_P}{L_g C\omega_s^2}-\frac{(4\lambda+2)\omega_r^2 L_m}{\omega_s}+\frac{\omega_s L_m}{(4\lambda+2)} \end{aligned} \quad (14)$$

According to (11) and (12), the effect of delay and grid side inductance on the value range of K_C to keep system stable can be depicted in Fig.3 based on the parameters shown in Table I. In Fig.3(a), it can be found that only when $\omega_r < \omega_c$, reducing delay can help expand the value range of K_C, which improve the system stability. But when $\omega_r > \omega_c$, compensating delay will narrow the value range of K_C and worsen the system stability.

Especially, when $\omega_r = \omega_c$, there is 'Threshold1 = Threshold2', which means the system is critical stable in this condition and this mathematically illustrates the reason why the system cannot keep stable no matter how the capacitor current coefficient is adjusted when $\omega_r = \omega_c$.[5]. On the other hand, in Fig.3(b), the resonant frequency ω_r decreases with the increase of grid inductance and the grid inductance will narrow the stable region when $\omega_r > \omega_c$ while improve the stable region when $\omega_r > \omega_c$. Similarly, '$\omega_r = \omega_c$' is a critical stable point.

Besides, it can be found that although active damping methods are adopted, the resonant peak still exists. But on the other hand, the active damping control and the delay both can provide damping in which the active damping control create zeros to provide phase lead while the delay provide phase lag. Therefore, the damping can be regarded as the phase adjustment at the resonant frequency. In fact, beside CCF active damping, the mechanism of other damping methods like capacitor voltage feedback active damping can also be explained like this, which keeps system stable by adjusting the phase of LCL resonance frequency.

IV. Simulation and Experimental Results

In order to verify the effectiveness of the derived equation (11) and (12) to judge the system stability. The simulation and experiment with the parameters listed in Table I are designed. It can be found that there is $f_r > f_c$, according to (12), the value range of K_C to keep system stable should be [-7.6049, 2.4658]. Therefore, the simulation and experiment are designed as follows

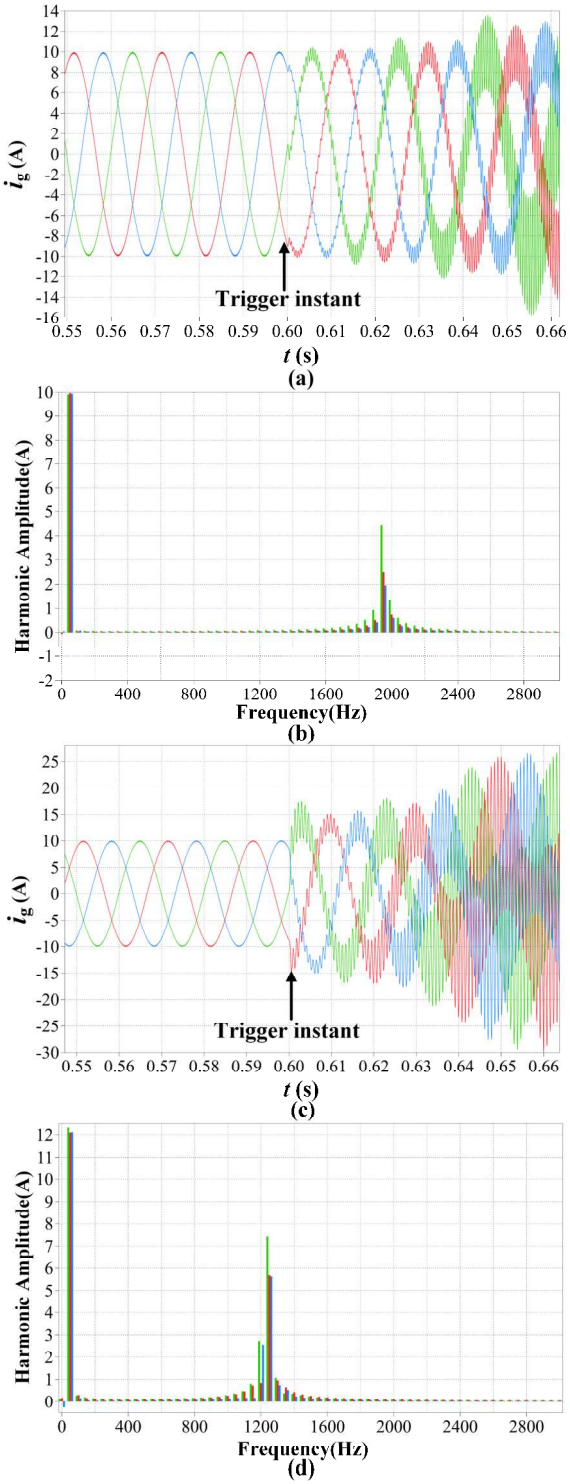

Fig. 4 Simulation results. (a) Grid current wave of Case 1. (b) Oscillation frequency analysis of (a). (c) Grid current wave of Case 2. (d) Oscillation frequency analysis of (c)

1)Case 1: K_C is set to change from 1 to 2.6 at 0.5s in the simulation and experiment.

2)Case 2: K_C is set to change from 1 to -7.8 at 0.5s in the simulation and experiment;

The simulation results are shown in Fig.4, in which Fig.4(a) and Fig.4(b) shows the grid current waveform

and oscillation frequency analysis of Case1. It can be found that the system turns unstable when K_C jumps from 1 to 2.6 and the oscillation frequency is around 1.95kHZ, which corresponds to the resonant frequency f_r. The instability in Case1 can be explained by Fig.2(d) that the change of K_C from 1 to 2.6 results in $f_r > f_0$ but the phase lag caused by delay is larger than the phase lead at f_0, leading to the -180° phase crossing at the resonant peak frequency f_r and presented as the oscillation around the frequency f_r. In Case 1, it is the phase lag of delay that cause instability thus Case1 shows the negative effect of delay on stability.

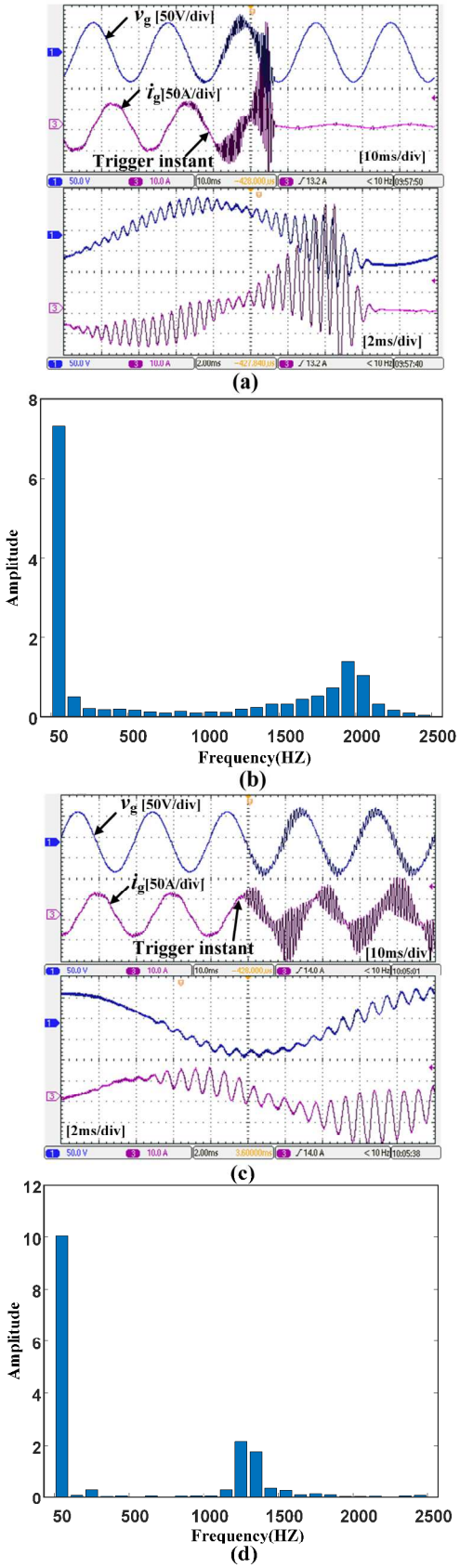

Fig. 5: Experiment results. (a) Experiment results of Case 1. (b) Oscillation frequency analysis of (a). (c) Experiment results of Case 2. (d) Oscillation frequency analysis of (c)

On the other hand, Fig.4(c) and Fig.4(d) shows the grid current waveform and oscillation frequency analysis of Case 2. Similarly, the oscillation occurs when K_C change from 1 to -7.8 but the oscillation frequency is around 1.25kHZ, corresponding to the frequency f_c. The instability in Case2 can be explained by Fig.2(c) that the change of K_C from 1 to -7.8 results in $f_r < f_0$ and the phase lag caused by delay help avoid -180° phase crossing at the resonant frequency f_r . Instead, the phase crosses -180° at the frequency f_c and the system can keep stable if the magnitude at f_c is less than 0dB. However, K_C < -7.8 makes the magnitude larger than 0dB at f_c, leading to the instability presented as the oscillation around the frequency f_c. In Case 2, the delay shows an positive effect on the system stability while the active damping control results in the instability, which proves the analysis that both the delay and active damping control can provide damping

The experimental results are shown in Fig.5 similar with the simulation results. Fig.5(a) and Fig.5(b) shows the gird current and voltage waveform and the current oscillation frequency analysis of Case1. The instability are presented as the oscillation around 1.95kHZ, which validates the simulation results of Fig.4(a) and Fig.4(b). Fig.5(c) and Fig.5(d) shows the gird current and voltage waveform and the current oscillation frequency analysis of Case2. The instability are presented as the oscillation around 1.25kHZ, which validates the simulation results of Fig.4(c) and Fig.4(d).

V. CONCLUSIONS

In this paper, a loop gain reconfiguration method is proposed to avoid system RHP poles caused by delay in the LCL-type grid-connected converters with CCF AD. Through the model, analytic expressions to judge the system stability are derived, It is found that both active damping control and delay can provide damping for the system through adjusting loop-gain phase around LCL resonance frequency. Furthermore, the effect of delay and grid impedance on the stable region are presented. It is shown that the stable region gets narrow and then expands with the increase of delay and grid impedance. The stable region is reduced to a value when the phase lag at LCL resonant frequency is equal to 90° and the system are critical stable. Finally, the simulation and experiment validate the analysis.

ACKNOWLEDGMENT

This paper is supported by the National Science Foundation of China (51977172).

REFERENCES

[1] M. Liserre, F. Blaabjerg, and S. Hansen, "Design and Control of an LCL-Filter-Based Three-Phase Active Rectifier," IEEE Transactions on Industry Applications, vol. 41, no. 5, pp. 1281-1291, 2005.

[2] R. Peña-Alzola, M. Liserre, F. Blaabjerg, R. Sebastián, J. Dannehl, and F. W. Fuchs, "Analysis of the Passive Damping Losses in LCL-Filter-Based Grid Converters," IEEE Transactions on Power Electronics, vol. 28, no. 6, pp. 2642-2646, 2013.

[3] B. Chenlei, R. Xinbo, W. Xuehua, L. Weiwei, P. Donghua, and W. Kailei, "Step-by-Step Controller Design for LCL-Type Grid-Connected Inverter with Capacitor–Current-Feedback Active-Damping," IEEE Transactions on Power Electronics, vol. 29, no. 3, pp. 1239-1253, 2014.

[4] D. Pan, X. Ruan, C. Bao, W. Li, and X. Wang, "Capacitor-Current-Feedback Active Damping With Reduced Computation Delay for Improving Robustness of LCL-Type Grid-Connected Inverter," IEEE Transactions on Power Electronics, vol. 29, no. 7, pp. 3414-3427, 2014.

[5] S. G. Parker, B. P. McGrath, and D. G. Holmes, "Regions of Active Damping Control for LCL Filters," IEEE Transactions on Industry Applications, vol. 50, no. 1, pp. 424-432, 2014.

[6] V. Miskovic, V. Blasko, T. M. Jahns, A. H. C. Smith, and C. Romenesko, "Observer-Based Active Damping of LCL Resonance in Grid-Connected Voltage Source Converters," IEEE Transactions on Industry Applications, vol. 50, no. 6, pp. 3977-3985, 2014.

[7] D. Pan, X. Ruan, C. Bao, W. Li, and X. Wang, "Optimized Controller Design for LCL-Type Grid-Connected Inverter to Achieve High Robustness Against Grid-Impedance Variation," IEEE Transactions on Industrial Electronics, vol. 62, no. 3, pp. 1537-1547, 2015.

[8] X. Wang, F. Blaabjerg, and P. C. Loh, "Virtual RC Damping of LCL-Filtered Voltage Source Converters With Extended Selective Harmonic Compensation," IEEE Transactions on Power Electronics, vol. 30, no. 9, pp. 4726-4737, 2015.

[9] S. Guoqiao, X. Dehong, C. Luping, and Z. Xuancai, "An Improved Control Strategy for Grid-Connected Voltage Source Inverters With an LCL Filter," IEEE Transactions on Power Electronics, vol. 23, no. 4, pp. 1899-1906, 2008.

[10] S. Guoqiao, Z. Xuancai, Z. Jun, and X. Dehong, "A New Feedback Method for PR Current Control of LCL-Filter-Based Grid-Connected Inverter," IEEE Transactions on Industrial Electronics, vol. 57, no. 6, pp. 2033-2041, 2010.

[11] N. He et al., "Weighted Average Current Control in a Three-Phase Grid Inverter with an LCL Filter," IEEE Transactions on Power Electronics, vol. 28, no. 6, pp. 2785-2797, 2013.

[12] J. Xu, S. Xie, and T. Tang, "Active Damping-Based Control for Grid-Connected LCL-Filtered Inverter With Injected Grid Current Feedback Only," IEEE Transactions on Industrial Electronics, vol. 61, no. 9, pp. 4746-4758, 2014.

[13] X. Wang, F. Blaabjerg, and P. C. Loh, "Grid-Current-Feedback Active Damping for LCL Resonance in Grid-Connected Voltage-Source Converters," IEEE Transactions on Power Electronics, vol. 31, no. 1, pp. 213-223, 2016.

[14] B. Liu, Q. Wei, C. Zou, and S. Duan, "Stability Analysis of LCL-Type Grid-Connected Inverter Under Single-Loop Inverter-Side Current Control With Capacitor Voltage Feedforward," IEEE Transactions on Industrial Informatics, vol. 14, no. 2, pp. 691-702, 2018.

[15] Y. He, X. Wang, X. Ruan, D. Pan, and K. Qin, "Hybrid Active Damping Combining Capacitor Current Feedback and Point of Common Coupling Voltage Feedforward for LCL-Type Grid-Connected Inverter," IEEE Transactions on Power Electronics, vol. 36, no. 2, pp. 2373-2383, 2021.

[16] J. Dannehl, M. Liserre, and F. W. Fuchs, "Filter-Based Active Damping of Voltage Source Converters With LCL Filter," IEEE Transactions on Industrial Electronics, vol. 58, no. 8, pp. 3623-3633, 2011.

[17] W. Yao, Y. Yang, X. Zhang, F. Blaabjerg, and P. C. Loh, "Design and Analysis of Robust Active Damping for LCL Filters Using Digital Notch Filters," IEEE Transactions on Power Electronics, vol. 32, no. 3, pp. 2360-2375, 2017.

[18] M. Wagner, T. Barth, R. Alvarez, C. Ditmanson, and S. Bernet, "Discrete-Time Active Damping of LCL-Resonance by Proportional Capacitor Current Feedback," IEEE Transactions on Industry Applications, vol. 50, no. 6, pp. 3911-3920, 2014.

[19] Z. Xin, X. Wang, P. C. Loh, and F. Blaabjerg, "Grid-Current-Feedback Control for LCL-Filtered Grid Converters With Enhanced Stability," IEEE Transactions on Power Electronics, vol. 32, no. 4, pp. 3216-3228, 2017.

[20] J. Yin, S. Duan, and B. Liu, "Stability Analysis of Grid-Connected Inverter with LCL Filter Adopting a Digital Single-Loop Controller with Inherent Damping Characteristic," IEEE Transactions on Industrial Informatics, vol. 9, no. 2, pp. 1104-1112, 2013.

[21] D. G. Holmes, T. A. Lipo, B. P. McGrath, and W. Y. Kong, "Optimized Design of Stationary Frame Three Phase AC Current Regulators," IEEE Transactions on Power Electronics, vol. 24, no. 11, pp. 2417-2426, 2009.